The vibrational relaxation of I_2 ($X\ ^1\Sigma_g^+$) in mesitylene

H. J. Liu, Stuart H. Pullen, Larry A. Walker II, and Roseanne J. Sension
Department of Chemistry, University of Michigan, Ann Arbor, Michigan 48109-1055

(Received 31 October 1997; accepted 22 December 1997)

Transient absorption measurements between 400 nm and 570 nm are used to extract information on the vibrational relaxation of iodine in the complexing solvent mesitylene. The well characterized nature of the I_2-arene complex makes it an excellent prototype for the study of relaxation processes in the presence of weak interactions. The data and analysis presented here demonstrate the rapid nonexponential vibrational relaxation of I_2 in the interacting solvent mesitylene. The peak of the population distribution has dropped below $n=10$ by 11 ps and $n=7$ by 15.5 ps. The energy relaxation is characterized by a biexponential decay with time constants of 4.41 ± 0.08 ps and 20.3 ± 0.7 ps. Quantitative comparisons of relaxation in a variety solvents are made by using a simple time-delay to peak absorption characterization of the relaxation. The initial 4.4 ps decay in mesitylene is significantly faster than the time scales for relaxation in noninteracting hydrocarbon solvents. The difference in the relaxation rate cannot be attributed to a change in vibrational frequency as the vibrational frequency of I_2 has only a small dependence on the solvent. It is suggested that the vibrational relaxation of I_2 in mesitylene through the high-lying levels is better characterized as an ''intramolecular'' vibrational energy redistribution process than relaxation to a solvent bath. The ultrafast vibrational relaxation occurs via the anharmonic coupling of the I–I stretching coordinate and the I-MST stretching coordinate of an I_2-MST complex. [S0021-9606(98)01912-6]

I. INTRODUCTION

The theory of energy transfer between solute and solvent in the condensed phase has been a consistent challenge for chemists, reflecting both the complexity of liquid systems and the ultrafast reaction dynamics involved. Development of a rigorous understanding of energy transfer processes will facilitate progress toward a more complete picture of chemical dynamics in solution. In this paper we analyze ultrafast pump–probe studies of the photodissociation, geminate recombination, and vibrational relaxation of I_2 in a complexing solvent, mesitylene (1,3,5-trimethylbenzene, MST), with emphasis on the vibrational relaxation of I_2 following geminate recombination. This system provides an excellent model for the study of solute–solvent interaction dynamics. There is a wealth of experimental data and theoretical simulations exploring the geminate recombination and vibrational relaxation of iodine and di-iodide as a function of solvent.[1–18] The background provided by these studies supplies a motivation to study relaxation dynamics in the more complex but complementary I_2-mesitylene system. The well characterized nature of the I_2-arene complex makes it an excellent prototype for the study of relaxation processes in the presence of weak interactions. The coupling of the I_2 vibrational motion to the solvent via a ground state charge-transfer interaction provides an efficient and distinctive channel for the relaxation of highly excited I_2 molecules. In this respect, the study of vibrational relaxation in I_2-arene complexes provides a link between relaxation in isolated diatomic molecules and relaxation in polyatomic systems.

A number of groups have investigated the vibrational relaxation dynamics of iodine in the condensed phase.[1–8] The vibrational relaxation of highly excited I_2 in nonpolar solvents appears to be dominated by the repulsive interaction between solvent and solute. These interactions, along with the $\sim 212\ cm^{-1}$ vibrational frequency of I_2 result in a slow relaxation (50 ps–200 ps in nonpolar or polar aprotic solvents, and nanoseconds in atomic solvents) characterized by nearly exponential energy decay.[2–6] The relaxation is substantially faster in the excited A/A' state (5–14 ps), an experimental observation attributed primarily to the lower vibrational frequency in this state ($106\ cm^{-1}$).[7] Harris and coworkers have reported comprehensive transient absorption studies on iodine in various solvents.[2–6] These studies extended the isolated binary collision (IBC) model for gas phase relaxation to the I_2/liquid Xe system and found reasonable consistency. For I_2 in alkane and chlorinated alkane solvents they deduced a ~ 15 ps relaxation time to the middle vibrational levels of the ground state and $\sim 150-200$ ps to reach the lowest vibrational levels. No evidence for significant vibration to vibration ($V-V$) energy transfer was found in chlorinated solvents. However, it was proposed that $V-V$ relaxation might be more important in alkane solvents.

Time-resolved resonance Raman spectroscopy was used by Hopkins and co-workers to provide more detailed information on the vibrational relaxation of I_2 in a variety of solvent environments.[7–8] The evolution of the Raman vibrational band suggests that the I_2 population has cooled to ca. $n=20$ by 25 ps following geminate recombination in *n*-hexane, cyclohexane, or cyclohexane-d_{12}.[8] The distribution is slightly cooler by 25 ps following geminate recombination in neo-hexane.[8] On the basis of these measurements, and measurements in dichloromethane, it was argued that the

$V-V$ relaxation channel is inefficient because of the lack of compatible solvent vibrational modes to accept excess energy. Simply having a vibrational mode of the proper frequency is insufficient, the solvent mode must be able to couple to the vibrational motion of the excited I_2 solute molecule. These investigators suggested that vibration to translation ($V-T$) and possibly vibration to rotation ($V-R$) mechanisms are the main channels for energy relaxation.

In contrast to the relaxation rates observed for neutral I_2 in solution, the vibrational relaxation of di-iodide (I_2^-) is incredibly fast and characterized by nonexponential energy decay. Relaxation to ca. $n=10-15$ requires less than 300 fs following dissociation and geminate recombination. This fast initial relaxation is followed by a slower 3–6 ps relaxation to thermal equilibrium with the surroundings. The difference in relaxation rate between I_2 and I_2^- is attributed to a lower vibrational frequency ($115\ cm^{-1}$) and to solvent-induced solute charge flow.[17,18] The electrostatic interaction between a charged solute and the polar solvent will provide a frictional drag on the vibrational motion. This is especially true in the higher vibrational levels, where the charge cannot remain symmetrically delocalized over both iodine atoms. Interaction with the solvent will tend to localize the charge on one of the iodine atoms. The frictional drag of the solvent transfers energy from the solute to the solvent resulting in rapid relaxation.

Dissociation of I_2 in mesitylene provides the opportunity to study vibrational relaxation in the presence of a specific I_2–solvent interaction. It is well known that the vibrational frequency of a diatomic halogen molecule is perturbed by complexation with an aromatic hydrocarbon. In the absence of a charge transfer (CT) interaction, the ground state vibrational frequency of I_2 is slightly dependent upon the solvent, varying from $213\ cm^{-1}$ in the gas phase to ca. $211\ cm^{-1}$ in noninteracting solvents (e.g., *n*-alkanes, cycloalkanes, carbon tetrachloride, and chloroform).[19–21] The frequency is reduced to ca. $205\ cm^{-1}$ in benzene, $204\ cm^{-1}$ in toluene, and $200\ cm^{-1}$ in mesitylene.[19]

The origin of the shift in the vibrational frequency of halogens in complexing solvents is twofold, with contributions from the general dielectric medium as well as a contribution from the specific charge-transfer interaction. The existence of a specific interaction has been demonstrated in the far-IR spectra of solutions containing IBr and benzene, toluene or *p*-xylene in *n*-decane. In these solutions vibrational bands corresponding to both complexed and uncomplexed IBr are easily distinguished at room temperature.[22,23] A similar pair of bands is observed in the low temperature resonance Raman spectrum of I_2 with benzene in *n*-heptane solvent.[24] The steady state 233 K resonance Raman measurements by Lascombe and co-workers demonstrate the presence of two vibrational bands centered at 211 and 208 nm with the lower frequency attributed to the complexed I_2 molecules. These investigators also used the temperature dependence of the vibrational bands to set a lower limit for the lifetime of an I_2-benzene complex at 0.7 ps near room temperature.

Several studies of the reaction dynamics of I_2-aromatic charge transfer complexes following laser excitation have been reported recently.[25–30] The reaction steps observed include charge transfer, bond breaking, recombination, and vibrational relaxation. Upon optical excitation in the CT band of I_2-arene complexes, photodissociation occurs along two primary reaction coordinates, I–I bond (forming I and I-arene) and I-arene bond (forming I_2 and arene).[26,27] It was pointed out in our previous paper that the spectral evolution observed in the visible region of the spectrum following excitation at 400 nm is characteristic of vibrational relaxation.[29] This signal dominates the transient absorption spectra obtained after 400 nm excitation, although it is much smaller, or nonexistent following excitation at 310 nm.[27,30] The difference may be attributed to a change in geminate recombination related to the photoproduct momentum as suggested earlier.[29] Alternatively, the difference between excitation at 310 nm and 400 nm may reflect a change in the primary photophysics. Excitation at 400 nm may result in internal conversion producing vibrationally excited ground state I_2 without complete dissociation and recombination. In either event, the vibrational relaxation component following excitation at 400 nm is unmistakable. This signal therefore provides the opportunity to study the vibrational relaxation of I_2 in an interacting solvent.

II. EXPERIMENT

The transient kinetic measurements analyzed here to describe the vibrational relaxation of I_2 in MST have been reported previously.[29] The new experimental result presented here is a transient absorption spectrum, obtained at a delay time of 200 ps following excitation at 400 nm. The femtosecond pump–probe apparatus used in this experiment has been described previously.[29] For the measurement of transient difference spectra, the setup was modified to use spherical mirrors at near normal incidence to collimate and focus the probe after continuum generation. This was done to minimize chromatic aberration resulting from refractive optics. The probe beam was rotated to vertical polarization and the pump beam was rotated to magic angle so that only isotropic data would be collected. The continuum and the pump pulse were focused to about 500 μm diameter. After passing through the sample, the probe beam was focused onto an optical fiber connected to a SPEX 500M spectrometer with a Princeton Instruments Model LN/CCD-1100-PB CCD camera. Each camera exposure was 250 ms in duration and 5000 exposures were collected. In order to obtain a difference spectrum a solenoid with a shutter was timed to block the pump beam every other time the camera shutter closed. The difference spectra were calculated by averaging every other exposure to obtain a pumped average while the remaining 2500 exposures were averaged to give a reference. Taking the common log of the ratio then gave the recorded spectra.

Samples were prepared by dissolving solid I_2 (Aldrich 99.9%) in mesitylene (Aldrich 99+%). The solutions had an I_2 concentration of ~ 0.01 M with about 85% of the I_2 complexed with MST and an optical density of ~ 0.8 at 400 nm for 1 mm path length.[29] The samples were kept in a reservoir at 11 °C and flowed through a quartz cell with a 1 mm path length. UV–Vis absorption spectra were recorded before and

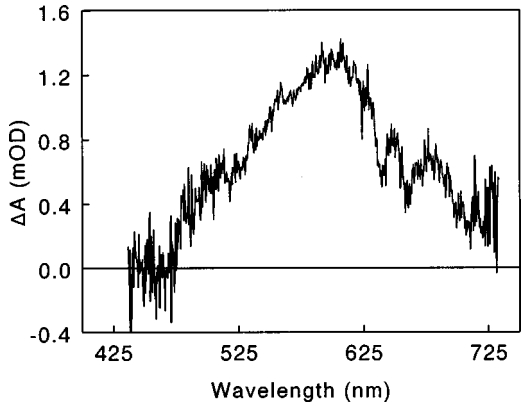

FIG. 1. Transient absorption spectrum obtained 200 ps following excitation of I_2 in mesitylene. The spectrum shown in this figure is a composite of three different spectra taken with windows from 436 nm to 613 nm, 472 nm to 647 nm, and 567 nm to 734 nm.

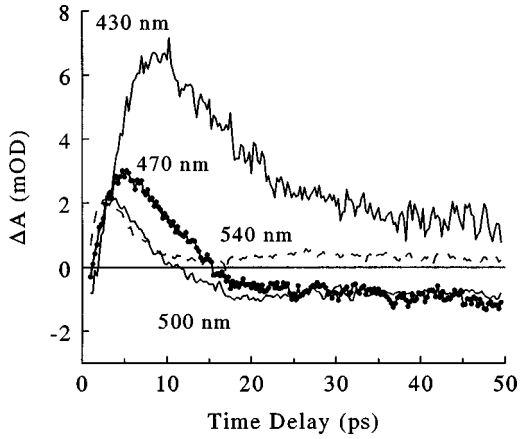

FIG. 2. Transient absorption signals attributed to the vibrational relaxation component following the excitation of I_2 in mesitylene at 400 nm. These data were extracted from the transient kinetics reported in Ref. 29 by using Eq. (1) and the I-MST spectrum shown in Fig. 1.

after each set of measurements, and a fresh sample was prepared immediately prior to measurement in order to avoid sample degradation.

III. RESULTS

Three overlapping spectral windows were combined to give rise to the difference spectrum shown in Fig. 1. This spectrum is qualitatively similar to those reported by Strong and co-workers,[31–33] Hilinski and Rentzepis,[26] and Raner *et al.*[34] The difference spectrum peaks around 600 nm and exhibits a broad positive absorption. The decrease on the blue side of the spectrum reflects both the absorption of I-MST and the bleaching of the visible I_2 absorption band. The actual I-MST absorption may peak at somewhat shorter wavelengths. The current spectrum covers the range from 470 nm to 730 nm. The measurements reported by Hilinski and Rentzepis suggest that the difference spectrum will level off, or even turn up slightly in the blue wing by 430 nm.[26]

The transient absorption signals probed in the kinetic measurements reported previously contain contributions from three separate difference spectra corresponding to the dissociation and recombination channels.[29] The total signal can be expressed as

$$S(t)=[2A_{\text{I-MST}}-A_{\text{I}_2\text{-MST}}][\phi_1 e^{-t/\tau_1}+\phi_2]+[A^{\text{HOT}}_{\text{I}_2\text{-MST}}(t) - A_{\text{I}_2\text{-MST}}]*[\phi_3+(1-e^{-t/\tau_1})\phi_1]+\Delta A_{\text{CT}}(t)\phi_4. \quad (1)$$

The first contribution to the total signal is the difference spectrum, $[2A_{\text{I-MST}}-A_{\text{I2-MST}}]$, for the formation of 2 I-MST complexes following dissociation of an I_2 molecule. This difference spectrum is determined experimentally from the 200 ps transient absorption spectrum. The quantity $(\phi_1+\phi_2)$ is the quantum yield for the initial formation of I-MST complexes and ϕ_2 is the quantum yield for ''permanent'' photoproduct formation. Recombination in this channel is well modeled with a single exponential decay using $\phi_1 \simeq \phi_2$ and $\tau_1 \approx 14.8$ ps. The second contribution to the total signal is the difference spectrum, $[A^{\text{HOT}}_{\text{I2-MST}}(t)-A_{\text{I2-MST}}]$ corresponding to the formation and relaxation of vibrationally hot ground state I_2 molecules. This difference spectrum is convoluted with the expression for the time-dependent repopulation of the ground state. The quantity ϕ_3 is the quantum yield for prompt (1–2 ps) geminate recombination while ϕ_1 is the quantum yield for delayed recombination. The magnitude of $\Delta A_{\text{CT}}(t)\phi_4$ represents the fast transients corresponding to dissociation of I_2-MST complexes to I_2+MST and the subsequent re-establishment of an equilibrium distribution of complexes. This latter channel has very little impact on the transient absorption signals probed between 430 nm and 750 nm, but complicates the analysis of the shorter wavelength data significantly. The analysis in this paper will concentrate on modeling the difference spectrum resulting from the recombination and vibrational relaxation of I_2 in mesitylene.

The I-MST difference spectrum obtained at 200 ps (Fig. 1) can be used to identify the vibrational relaxation component in the kinetic data between 430 nm and 600 nm. Subtraction of the I-MST difference spectrum from the transient absorption data leaves the signal due to I_2 recombination and vibrational relaxation, as well as a fast component attributed to the dissociation of I_2-MST complexes along the CT bond. Both prompt recombination and recombination from I-MST are included. The isolated kinetic data containing the signal attributed to vibrational relaxation is shown in Fig. 2 for wavelengths between 430 nm and 540 nm.

IV. MODEL CALCULATIONS

A. Electronic state potentials

A detailed analysis of the vibrational relaxation process requires a model for the absorption spectrum as a function of vibrational excitation. For the present analysis of the I_2-MST complex three electronic states (the ground state, the CT state, and the local B state of I_2) must be included to model the observed absorption spectrum. The A and B'' states also contribute to the experimentally observed ground state absorption spectrum, but these contributions are small and may be neglected without compromising the overall accuracy of the analysis.

The I_2-MST complex may be approximated as a triatomic molecule (MST-I-I) comprised of three ''atoms'' of approximately equal mass. The molecular weight of MST is 120 amu while the atomic mass of an iodine atom is 127 amu. There are three vibrational coordinates in the ''triatomic'' complex, an I-MST bond length, and I–I bond length, and a bending coordinate. An axial complex, with the I–I bond oriented in a direction perpendicular to the aromatic plane would have two degenerate bending coordinates. Recent work by Lenderink *et al.*,[30] and by Young and co-workers,[35,36] suggests that an I_2-aromatic complex has an oblique geometry with a shallow minimum at $\sim 30°$ with respect to the perpendicular axial geometry. The transition moment of the CT transition is strongly dependent on the angle that the I_2 molecule makes with the plane of the aromatic donor.[30] Therefore photoinduced perturbations in this angle could influence the transient absorption spectra as equilibrium is re-established. However, molecular dynamics simulations of I_2-benzene complexes suggest that this angle is dynamic in solution phase complexes.[30,37] An equilibrium distribution of angles should be reestablished quickly. In the discussion which follows we shall model the I_2-MST complex with two one-dimensional stretching coordinates, and ignore the bending angle. This is a reasonable approximation because we are modeling vibrational relaxation primarily on time scales longer than a few picoseconds.

In this paper, we will model the I-MST and I–I coordinates of the ground and excited electronic states of I_2-MST with Morse potentials, with the exception of the excited state I-MST coordinate, which will be modeled with a Coulomb attractive and $1/r^{12}$ repulsive potential. The Morse oscillator potential has a functional form,

$$V(r)=D\{1-e^{-\beta(r-r_e)}\}^2+V_0. \tag{2}$$

The vibrational energy levels of a Morse oscillator are described by

$$E(n)=\frac{\omega_e}{2\pi c}\left[\left(n+\frac{1}{2}\right)-\frac{1}{2\gamma}\left(n+\frac{1}{2}\right)^2\right], \tag{3}$$

where the ''harmonic'' frequency ω_e is related to the potential parameters by

$$\omega_e=\sqrt{\frac{2Dhc\beta^2}{\mu}}, \tag{4}$$

and the anharmonicity is related to

$$\gamma=\frac{4\pi Dc}{\omega_e}. \tag{5}$$

The potential parameters are listed in Table I. The parameters for the ground and excited B states of I_2' are from Refs. 1 and 38. The I–I bond in the CT state is approximated by using the ground state I_2^- potential from Ref. 39.

The iodine $B \leftarrow X$ transition usually peaks around 520 nm in gas phase or inert solvents.[40] In mesitylene, the iodine visible absorption is blue shifted to peak at 490 nm, indicating a ~ 0.16 eV energy shift on the B state potential with respect to that of the X ground state. The minimum energy (V_0) of the B-state potential is optimized to fit the absorption spectrum.

TABLE I. Potential surface parameters used in the analysis of I_2 relaxation.

State	D (cm^{-1})	β ($Å^{-1}$)	r_e (Å)	V_0 (cm^{-1})
X (I–I)	12 547.2	1.75	2.67	0
X or B (I-MST)	1 043.2	1.55	3.88	···
B (I–I)	4 381.8	1.75	3.03	17 068
CT (I–I)	8 871.5	1.16	3.23	18 880
State	A (cm^{-1} $Å^{12}$)	B (cm^{-1} Å)	C (cm^{-1})	
CT (I-MST)	3.137×10^9	1.0445×10^5	2.9921×10^4	

The I-MST potentials are presented in Fig. 3. The ground state potential energy has rarely been described because of the experimental difficulties in the vibrational study of such a heavy, weakly bonded complex. The jet spectroscopy studies by McLean *et al.*[41] on I_2-benzene estimated the binding energy of I_2-Bz was about 770 cm^{-1}. Theoretical calculations also suggest a weak ground state binding energy for the I_2-Bz complex.[37,42–44] Based on the ~ 0.125 eV heat of formation for I_2-MST, a ground state binding energy of ~ 1040 cm^{-1} is estimated.[45–48] The equilibrium separation between iodine and benzene were estimated by *ab initio* calculations performed with the GAUSSIAN 94 program.[49] The equilibrium separation is estimated to be 3.88 Å between the center of the aromatic ring and the center of the closest iodine atom. This is consistent with the assumptions of other workers, and with the sum of the van der Waal's radii of an iodine atom (2.15 Å) and a carbon atom (1.7 Å).

The I-MST potential in the CT state is constructed by combining a $1/r$ Coulombic attraction term with a $1/r^{12}$ repulsion term,

$$V(r)=\frac{A}{r^{12}}-\frac{B}{r}+C. \tag{6}$$

The potential minimum is at $r_{\text{I-MST}}=3.2$ Å and the dissociation energy is ~ 3.7 eV. The binding energy is estimated

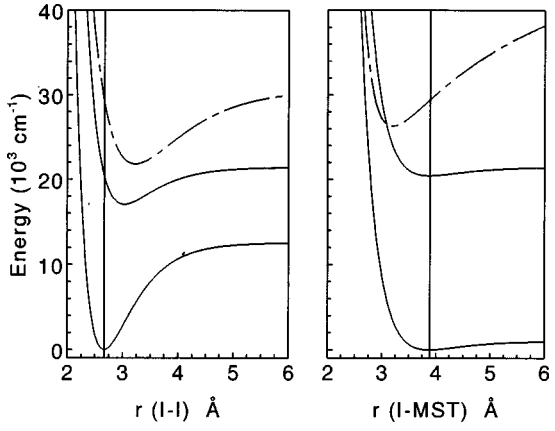

FIG. 3. Potential energy curves used to calculate the absorption spectrum of I_2 in mesitylene as a function of vibrational level.

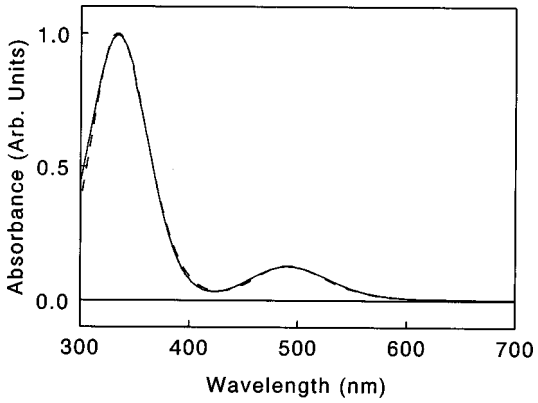

FIG. 4. Comparison of the calculated (dashed line) and experimental (solid line) equilibrium absorption spectra of I_2 in mesitylene at 284 K.

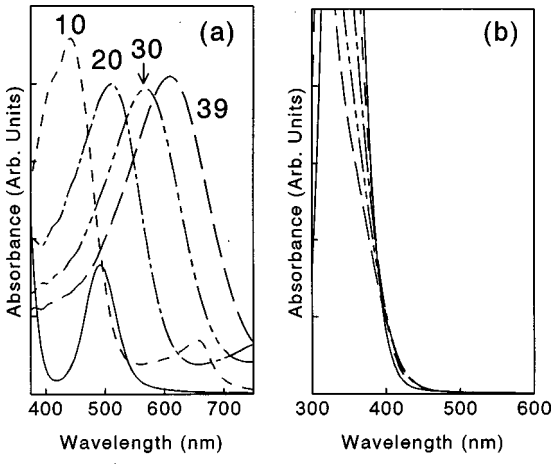

FIG. 5. (a) Absorption spectra calculated as a function of I–I vibrational level assuming an equilibrium distribution in the I-MST coordinate. The solid line is the equilibrium spectrum. (b) Absorption spectra calculated as a function of I-MST vibrational level assuming an equilibrium distribution in the I–I coordinate. The solid line is the equilibrium spectrum.

from the results of ~ 3.1 eV for I_2-Bz.[50] The CT potential energy curves along both coordinates are consistent with the parameters used by Cheng *et al.*[51,52]

The detailed features of the I_2-MST potential energy surface discussed above are only approximate. However, the data analyzed here is sensitive primarily to the slope of the I_2^- potential curve in the Franck–Condon region, as well as to the lowest 20 or so vibrational levels of the ground electronic state. This region is modeled reasonably well by the potential energy surfaces described above.

B. Absorption cross sections

Absorption spectra are calculated as a function of frequency and initial vibrational level (a,b) according to

$$\sigma_{a,b}(\nu)=\frac{8\pi^3\nu}{3}\sum_E \frac{g_E}{g_X}|\mu_{XE}|^2\frac{\Gamma_E}{\pi hc} \times \sum_{m_E,n_E}\frac{|\langle n_E|a\rangle|^2|\langle m_E|b\rangle|^2}{(E_{n_E}-E_a+E_{m_E}-E_b+\Delta\epsilon_E-\nu)^2+\Gamma_E^2}, \tag{7}$$

where a,b are the initial vibrational levels in the I–I and I-MST coordinates, respectively, n_E, m_E are the vibrational levels of the excited electronic states along the same coordinates, g_E and g_x are the degeneracies of the electronic states, Γ_E is a phenomenological homogeneous line width for each electronic state, $\Delta\epsilon_E$ is the energy separation between the minima of the ground and excited electronic state potential energy surfaces.

The ground and excited state vibrational wave functions are calculated by using the algorithm described in Ref. 38 (with several typographical errors corrected).[53] The unbound excited state wave functions are calculated by implementing the WKB approximation with Airy function patching across the classical turning point.

The equilibrium absorption spectrum was calculated by using

$$\sigma(\nu)=\sum_{a,b}P_{a,b}\sigma_{a,b}(\nu), \tag{8}$$

where $P_{a,b}$ is the Boltzmann population distribution for $T=284$ K. In all of the present calculations the transition dipole moment, μ_{XE}, is assumed to be independent of r. Using a Lorentzian broadening factor of 115 cm^{-1}, and wave functions for the potentials described above (see Table I), we get very good agreement between the calculated I_2-MST spectrum and the experimental result as shown in Fig. 4.

To explore the effect of vibrational relaxation on the observed absorption spectrum we have calculated absorption spectra (a) as a function of I–I vibrational level with a room temperature population distribution in the I-MST coordinate and (b) as a function of I-MST vibrational level with a room temperature population distribution in the I–I coordinate. The results are shown in Fig. 5. The hot spectra along the I-MST channel [Fig. 5(b)] show limited broadening on the blue side (not pictured) and almost no broadening on the red side. The shallow $1/r$ potential along the attractive part of the CT potential energy curve limits the sensitivity of the absorption spectrum to excess vibrational energy in the ground electronic state. Unless the form of the excited state surface differs substantially from that assumed here, vibrational relaxation along the I-MST coordinate will not influence the signal at wavelengths longer than ~ 400 nm, and thus cannot account for the transient absorption kinetics observed for I_2 in MST. On the other hand the absorption spectrum is very sensitive to excitation in the I–I bond, reflecting the steep slope of the excited state potential energy surface in the Franck–Condon region. Cooling in the I–I coordinate is responsible for the relaxation dynamics observed in the present set of measurements.

The data shown in Fig. 2 represent the vibrational relaxation along the I–I coordinate. The relaxation will be modeled by using

$$\Delta A(t)=[A^{\mathrm{HOT}}_{\mathrm{I_2\text{-}MST}}(t)-A_{\mathrm{I_2\text{-}MST}}] =\left[\sum_n(\sigma_n(\nu)-\sigma^{\mathrm{eq}}(\nu))\cdot P_n(t)\right], \tag{9}$$

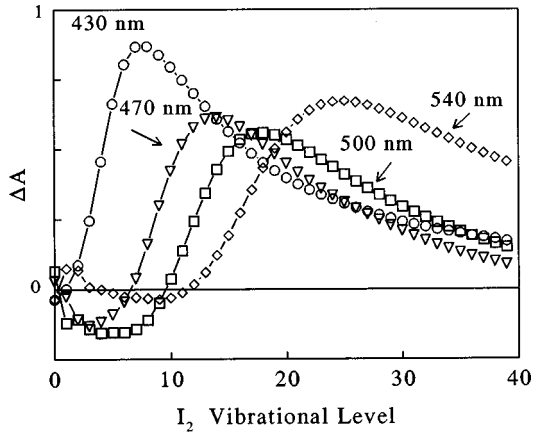

FIG. 6. Change in absorbance calculated for four probe wavelengths assuming that the population is removed from an equilibrium distribution and placed into a given vibrational level [see Eq. (10)].

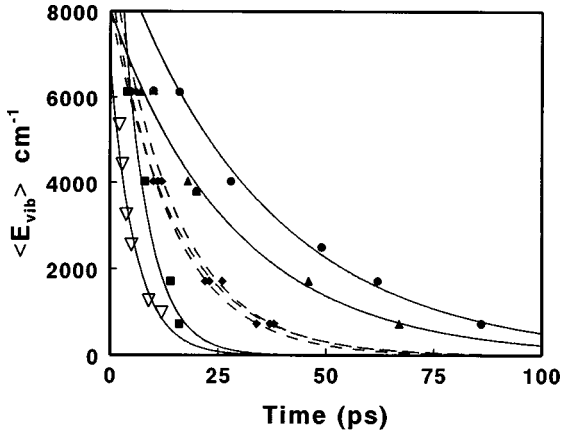

FIG. 7. Average excess vibrational energy as a function of time for I_2 in a variety of solvents as characterized by the time delay to peak absorption in the transient absorption measurements. The open triangles represent the time delay to peak absorption for I_2 in mesitylene at probe wavelengths between 400 nm and 570 nm. Each wavelength is assigned to an average excess energy by using the maxima observed in ΔA as a function of vibrational level as plotted in Fig. 6. The filled symbols represent the time delay to peak absorption for I_2 in CH_2Cl_2 (squares), *n*-hexane, *n*-nonane, and *n*-hexadecane (diamonds), cyclohexane (triangles), and carbon tetrachloride (circles) as reported in Ref. 2 (Table III and Figs. 16 and 17). The lines through the data points represent exponential fits to the data.

where $\sigma^{eq}(\nu)$ is the absorption cross section as a function of frequency for an ensemble of I_2 molecules in mesitylene at 284 K and $\sigma_n(\nu)$ is the absorption cross section as a function of frequency for an ensemble of I_2 molecules all in vibrational level n. The quantity $(\sigma_n(\nu)-\sigma^{eq}(\nu))$ therefore represents the difference spectrum obtained for placing an ensemble of I_2 molecules at 284 K into vibrational level n. $P_n(t)$ is the population of each vibrational level as a function of time following excitation. In our analysis of vibrational relaxation we have included the vibrational levels $n=0$ to $n=38$. Relaxation through the higher-lying vibrational levels is sufficiently rapid ($\ll 1$ ps) that explicit inclusion is not warranted.

It is informative to plot the expected difference signal as a function of ground state vibrational energy level. This difference is given by

$$\Delta A_\nu(n)=(\sigma_\nu(n)-\sigma_\nu^{eq}), \tag{10}$$

where ν is the wavelength of the transient absorption measurement, and n is the ground state vibrational energy level. This function is plotted in Fig. 6 for probe wavelengths of 430 nm, 470 nm, 500 nm, and 540 nm. As expected, the shorter wavelengths are more sensitive to the lower vibrational levels of the ground state while the longer wavelengths are more sensitive to the higher energy levels. Comparison of the plots in Fig. 6 and Fig. 2 demonstrates the rapid vibrational relaxation observed for hot I_2 in MST. By 10 ps the ensemble has cooled to the lower part of the I_2 well. The zero crossing points in the data obtained at 500 nm (11.5 ps) and 470 nm (15.5 ps) correspond to population distributions dropping below ca. $n=10$ and $n=7$, respectively. The slow decay at longer times arises from the recombination of I_2 (from I-MST complexes) on a 15 ps time scale, as well as a decrease in the vibrational relaxation rate in the lower part of the well.

A theoretical understanding of the dynamics of the vibrational relaxation of I_2 in mesitylene provides a new challenge. Although there is no net charge on the I_2 molecule the vibrational relaxation is much faster than that observed for I_2 in noninteracting solvents. The results discussed above demonstrate that the peak of the population distribution has dropped below $n=10$ by 11 ps and $n=7$ by 15.5 ps. By contrast the I_2 population has only cooled to ca. $n=20$ by 25 ps following geminate recombination in *n*-hexane, cyclohexane or cyclohexane-d_{12}.[8] This difference in the relaxation rate is not influenced substantially by the change in vibrational frequency, as the vibrational frequency of I_2 in mesitylene is only slightly lower than the vibrational frequency in noncomplexing solvents such as cyclohexane, hexane, and carbon tetrachloride. Rather the relaxation serves as a probe of the specific solvent–solute interaction.

A more direct comparison of vibrational relaxation in mesitylene with relaxation in noninteracting solvents is possible. In their paper on the vibrational relaxation of I_2, Harris *et al.* tabulated the delay to maximum absorption observed for I_2 in a variety of solvents at several different wavelengths.[2] These investigators also estimated average energy distributions (i.e., vibrational energy levels) probed at the same wavelengths. This data is displayed in Fig. 7 along with a similar characterization of the vibrational energy relaxation observed in the present work with mesitylene solvent. Vibrational relaxation of iodine in mesitylene is much faster than relaxation in any of the other hydrocarbon solvents. Only relaxation in the polar dichloromethane solvent approaches the rate observed in mesitylene.

The transient absorption data contain more detailed information on vibrational relaxation than is characterized by the delay to peak time constant alone. Modeling the full vibrational decay transients leads to a much more complete understanding of the relaxation process and demonstrates the essential nonexponential character of the energy relaxation. The following section explores the vibrational relaxation process by modeling the complete transients.

C. Master equation approach

In this section we will use a master equation approach to extract rate information from the observed vibrational relaxation. The population master equation describing the relaxation of I_2 in the ground state vibrational manifold is

$$\dot{P}_n(t) = -\sum_m k_{n\to m} P_n(t) + \sum_m k_{m\to n} P_m(t), \tag{11}$$

where the sum over m is over all vibrational levels of the system, $P_i(t)$ is the population of level i at time t, and $k_{j\to i}$ is the state-to-state transition rate from vibrational level j to vibrational level i. Consideration of the detailed balance condition requires that

$$\frac{k_{n\to m}}{k_{m\to n}} = e^{-[\hbar(\omega_m-\omega_n)]/k_BT} = e^{-(\hbar\omega_{mn}/k_BT)}, \tag{12}$$

where $\hbar\omega_n$, $\hbar\omega_m$ are the vibrational energies in states n and m, T is the temperature, and k_B is the Boltzmann constant. The initial condition for the present problem includes instantaneous population of a dark state, a rate for prompt geminate recombination to the vibrational energy level $n=38$ and a rate for the delayed geminate recombination of I-MST to $n=38$.

In order to draw a connection between the observed spectral evolution and the mechanism of energy transfer between solute and solvent in the condensed phase it is necessary to develop a model for the rate constants, $k_{n\to m}$, describing the probability for a transition from state n to a lower energy state m. The rate constant for a given transition is proportional to a coefficient defined by

$$\gamma_{n\to m} = |\langle n|Q_{nm}|m\rangle|^2 G(\omega_{nm}), \tag{13}$$

where Q_{nm} is the reduced coordinate,

$$Q_{nm} = \sqrt{\frac{\mu\omega_{nm}}{\hbar}}\, r, \tag{14}$$

μ is the reduced mass of I_2, and $G(\omega)$ is a frequency dependent rate reflecting the power spectrum of the solvent (i.e., the ability of a solvent collision or the availability of a solvent mode to accept energy at a frequency ω).

For a harmonic oscillator, $\omega_{n+1,n}=\omega_{n+1}-\omega_n$ is a constant and only transitions between adjacent vibrational levels are allowed ($\langle n|r|m\rangle \neq 0$ only if $n=m\pm 1$). Under these conditions the transition rate between adjacent levels is linearly dependent upon the initial vibrational quantum number n, resulting in an exponential decay of the excess energy,

$$\gamma_{n\to n-1} = n\,\gamma_{1\to 0}. \tag{15}$$

On the other hand, an anharmonic oscillator will have $\omega_n - \omega_{n+1}$ dependent on n, this will allow the possibility of multiple quantum transitions and will also result in a nonexponential decay of the excess energy. In the present case, the potential surface is sufficiently ''harmonic'' for vibrational levels from $n=0$ to 20 that the multiquantum transition probability is too low to account for any significant energy relaxation. The present data set does not allow explicit conclusions to be drawn for vibrational levels above ca. $n=20$. Therefore, the problem may be simplified by including only transitions with $\Delta n=1$. However, the anharmonicity is still sufficient to result in a nonexponential energy decay, augmented by the effect of $G(\omega)$ on the transition rates.

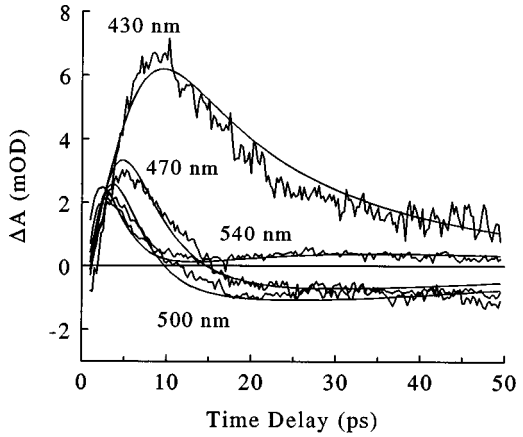

FIG. 8. Comparison of the experimental transient absorption signals with the best fit calculated according to Eq. (11) by using rate constants given by Eqs. (13) and (17). The fitting parameter was $G(\omega)$.

For a given anharmonic oscillator, $G(\omega)$ is the fitting parameter available to model the observed transient absorption signals. For relaxation dominated by hard collisions, the forward and backward rate constants are given by

$$k_{n\to m} = \gamma_{nm}, \quad k_{m\to n} = \gamma_{nm} e^{-\hbar\omega_{nm}/k_BT}. \tag{16}$$

In this case $G(\omega)$ is a frequency dependent rate reflecting both the collision frequency and the ability of a solvent collision to accept energy at a frequency ω. This approach is similar to the collisional energy relaxation model commonly used in the gas phase. Under the assumption that $V-V$ energy transfer is insignificant, $G(\omega)$ is expected to be approximately constant.

Another model, which also satisfies the detailed balance condition, considers the coupling of the anharmonic oscillator with a harmonic solvent bath.[54] The interaction induced damped anharmonic oscillator relaxation model treats the whole solvent bath as a collection of harmonic oscillators with various frequencies. Each of the solvent modes can be coupled to the hot solute as an energy recipient. In this model the forward and reverse rate constants are given by[54]

$$k_{n\to m} = \gamma_{nm}[\overline{n}(\omega_{nm})+1], \quad k_{m\to n} = \gamma_{nm}[\overline{n}(\omega_{nm})], \tag{17}$$

where $\overline{n}(\omega_{nm})$ is the boson occupation number for the solvent modes which are available to accept energy from the solute,

$$\overline{n}(\omega_{nm}) = [e^{\hbar\omega_{nm}/k_BT}-1]^{-1}. \tag{18}$$

For comparison with Eq. (16), Eq. (17) may be rewritten as

$$\begin{aligned} k_{n\to m} &= \gamma_{nm}[\overline{n}(\omega_{nm})+1], \\ k_{m\to n} &= \gamma_{nm}[\overline{n}(\omega_{nm})+1]e^{-\hbar\omega_{nm}/k_BT}. \end{aligned} \tag{19}$$

In this case $G(\omega)$ is a frequency dependent rate reflecting the availability of a solvent mode to accept energy at a frequency ω.

The best fit of the kinetic data to the master equation [Eq. (11)] is shown in Fig. 8. The $G(\omega)$ deduced from the fit

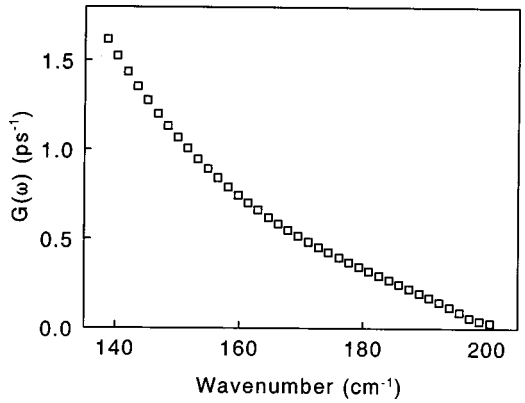

FIG. 9. Functional form of $G(\omega)$ used to fit the data as presented in Fig. 8.

according to Eqs. (17)–(19) is shown in Fig. 9. The transition rate is strongly dependent upon frequency resulting in a highly nonexponential decay of the energy. The best fit obtained with a constant $G(\omega)$ (i.e., nearly exponential energy decay) is shown in Fig. 10. This fit reproduces the time delay to peak absorption reasonably well, but does not reproduce the overall temporal behavior of the transient absorption signals, or even the relative intensities of the signals at different wavelengths very well at all.

The energy decay as a function of time is calculated from the master equation modeling of the transient absorption data according to

$$\langle E_{\mathrm{vib}}^{\mathrm{excess}}(t)\rangle + \langle E_{\mathrm{vib}}^{\mathrm{equil}}\rangle = \frac{\Sigma_n P_n(t) E_n}{\Sigma_n P_n(t)}, \tag{20}$$

where $P_n(t)$ is the population of each vibrational level considering only the prompt recombination channel. The excess energy decay obtained master equation model providing the best fit to the transient absorption data are plotted in Fig. 11, and compared with that deduced from the simple delay to peak of the transient absorption data. The delay to peak characterization of the vibrational energy relaxation appears to

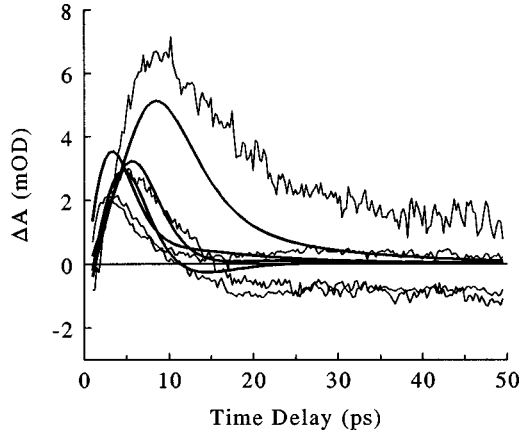

FIG. 10. Best fit to the transient absorption data obtained while holding $G(\omega)$ constant. This represents the best fit obtained assuming approximately exponential decay of the excess energy. For this fit $G(\omega)=0.44\ \mathrm{ps}^{-1}$. Note that the fit reproduces the delay to peak fairly well, but does not model the relative intensities or the detailed temporal behavior of the kinetic signals very well.

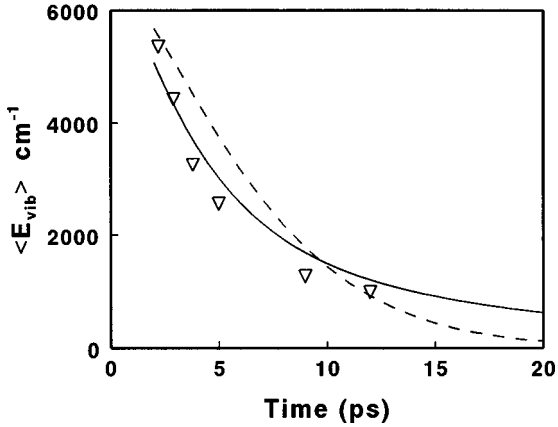

FIG. 11. The excess vibrational energy as a function of time for I_2 in mesitylene as inferred from three different methods of modeling, or characterizing, the data. The energy decays shown are as characterized by the time delay to peak absorption (open triangles), as calculated by using Eq. (20) for the best master equation model for the data (solid line), and as calculated by using the best fit to the data with $G(\omega)=$constant (dashed line).

provide a good semiquantitative model for the energy relaxation time scale. However, more detailed information is obtained from the complete master equation modeling of the data. In particular details such as nonexponentially are obscured in the simple delay to peak characterization.

V. DISCUSSION

The data and analysis presented here demonstrate the rapid nonexponential vibrational relaxation of I_2 in the interacting solvent mesitylene. Although there is no net charge on the I_2 molecule, the vibrational relaxation is much faster than that observed for I_2 in noninteracting solvents. The results presented above demonstrate that the peak of the population distribution has dropped below $n=10$ by 11 ps and $n=7$ by 15.5 ps. By contrast the I_2 population has only cooled to ca. $n=20$ by 25 ps following geminate recombination in *n*-hexane or cyclohexane.[8] Comparisons between solvents can be made more quantitative by contrasting time constants for exponential fits to the vibrational energy decay as characterized by the delay to peak data in Fig. 7. These exponential time constants (τ_c) are summarized in Table II. The characteristic time scale for energy relaxation in mesitylene is 4.5 ± 0.5 ps, significantly faster than the 7.5 ps time scale estimated for dichloromethane and much faster than the 13.5–25 ps time scales for relaxation in noninteracting hydrocarbon solvents. The difference in the relaxation rate is not influenced substantially by the change in vibrational frequency. The vibrational frequency of I_2 in mesitylene is only slightly lower than the vibrational frequency in the noncomplexing solvents.

Several recent papers have investigated the vibrational relaxation of di-iodide in a series of polar and nonpolar solvents.[11–18] Barbara and co-workers investigated the relaxation of I_2^- in a number of solvents including benzene.[17] Comparison of the present result for the relaxation of I_2 in mesitylene with the relaxation of I_2^- in benzene may be enlightening. In Walhout *et al.* the vibrational relaxation is characterized by using a biexponential description of the de-

TABLE II. Comparison of exponential and biexponential models for excess energy decay.

Solvent	Exponential fit τ_c (ps)	Bi-exponential fit A_1 (cm^{-1})	τ_1 (ps)	A_2 (cm^{-1})	τ_2 (ps)
Mesitylene[a]	4.5±0.5	5973±62	4.41±0.08	1482±73	20.3±0.7
Benzene (I_2^-)[b]		~1800	78±9 fs	~1400	1.8±0.1
n-alkanes[c]	13.5±1				
Cyclohexane[c]	25±3				
CCl_4[c]	33±5				
CH_2Cl_2[c]	7.5±1				

[a]The single exponential fit is obtained by fitting the ''delay to peak'' data as plotted in Fig. 7. The biexponential fit is obtained by fitting the decay of the excess energy obtained from the master equation model of the transient absorption data (plotted as the solid line in Fig. 11).
[b]Fit to the excess energy decay reported by Walhout *et al.* in Ref. 17.
[c]Time constant reported is for a fit to the excess energy decay displayed in Fig. 7 derived from ''delay to peak'' data reported in Ref. 2.

cay of excess energy.[17] The excess energy decay behavior calculated from the best fit to the I_2-MST transient absorption data (i.e., the solid line in Fig. 11) is well modeled as a biexponential decay. The exponential time constants for excess energy decay of I_2 in mesitylene and I_2^- in benzene are compared in Table II.

Much of the rate increase between the decay of iodine in mesitylene and the decay of di-iodide in benzene may be accounted for by the vibrational frequency decrease. This is particularly true for the longer decay component reflecting relaxation near the bottom of the potential well. Although a direct detailed comparison between I_2 in mesitylene and I_2^- in benzene is difficult, a molecular dynamic simulation by Danten *et al.* exploring I_2 in benzene may shed some light on the subject.[37] The power spectrum for I_2 in benzene obtained from the MD simulation indicates that the frequency dependent rate, $G(\omega)$, reflecting the availability of a solvent mode to accept energy at a frequency ω, should increase by approximately an order of magnitude as the vibrational frequency decreases from 200 cm^{-1} to 115 cm^{-1}. Assuming that mesitylene and benzene are comparable solvents, the frequency change alone may account for the 20 ps decay component for I_2 in mesitylene compared with the ca. 2 ps decay component for I_2^- in benzene. The initial fast energy decay, on the other hand, appears to be more sensitive to the details of the interaction between solute and solvent.

The initial rapid relaxation of I_2^- in benzene and other solvents is attributed to solvent-induced solute charge flow which gives rise to a particularly dramatic vibrational coordinate dependence to the solvent friction on the vibrational motion.[17,18] In the present investigation of I_2 in mesitylene, the energy relaxation through the high-lying vibrational levels is better thought of in terms of an intramolecular vibrational energy redistribution process. In the model of I_2-MST as a triatomic ''molecule,'' ultrafast vibrational relaxation occurs via the anharmonic coupling of the I–I stretching coordinate with the I-MST stretching coordinate of an I_2-MST complex. In the present investigation I_2 is diluted into neat mesitylene solvent. Thus each I_2 molecule may interact with more than one mesitylene molecule during the course of vibrational relaxation. The ultrafast vibrational relaxation of I_2 as a probe of the I_2-arene potential interaction using dilute complexes in a noninteracting solvent is a subject for a more detailed future investigation.

VI. CONCLUSIONS

Iodine undergoes a rapid nonexponential vibrational relaxation following geminate recombination in the interacting solvent mesitylene. The vibrational relaxation is much faster than that observed for I_2 in noninteracting solvents. The results presented above demonstrate that the peak of the population distribution has dropped below $n=10$ by 11 ps and $n=7$ by 15.5 ps. The data were analyzed in terms of a master equation model where the solvent bath is treated with a collection of harmonic oscillators with various frequencies, each of which can be coupled to the hot solute as an energy recipient. An appropriately chosen frequency dependent rate of relaxation, $G(\omega)$, allowed reproduction of the overall spectral behavior including the temporal behavior and relative intensities of individual transients obtained at several wavelengths. The relative intensities of the transient kinetics provided a much tighter constraint on the form of $G(\omega)$ than provided by the time dependence alone.

The fit of the master equation model to the data allowed recovery of a decay curve for the excess energy as a function of time. The excess energy decay is distinctly biexponential with time constants of 4.4 ps and 20 ps. It was also determined that the simple characterization of vibrational energy relaxation by the delay to peak absorption as a function of wavelength provides good semiquantitative agreement with the more exact calculations. The ultrafast initial relaxation of I_2 is attributed to anharmonic coupling between the I–I and I-MST ''local modes'' of an I_2-MST complex.

ACKNOWLEDGMENTS

This work was supported by a grant from the NSF (CHE-9415772). S.H.P. is supported by the NSF through the Center for Ultrafast Optical Science, under NSF Grant No. STC PHY 8920108. We would also like to acknowledge Dr. Joseph Shiang for valuable discussions.

[1] D. J. Nesbitt and J. T. Hynes, J. Chem. Phys. **77**, 2130 (1982).
[2] A. L. Harris, M. Berg, and C. B. Harris, J. Chem. Phys. **84**, 788 (1986).
[3] J. K. Brown, D. J. Russell, D. E. Smith, and C. B. Harris, Rev. Phys. Appl. **22**, 1787 (1987).
[4] J. K. Brown, C. B. Harris, and J. C. Tully, J. Chem. Phys. **89**, 6687 (1988).
[5] M. E. Paige and C. B. Harris, Chem. Phys. **149**, 37 (1990).
[6] D. J. Russell and C. B. Harris, Chem. Phys. **183**, 325 (1994).
[7] R. Lingle, Jr., X. Xu, S. Yu, H. Zhu, and J. B. Hopkins, J. Chem. Phys. **93**, 5667 (1990).
[8] X. Xu, S. Yu, R. Lingle, Jr., H. Zhu, and J. B. Hopkins, J. Chem. Phys. **95**, 2445 (1991).
[9] R. Zadoyan, Z. Li, P. Ashjian, C. Martens, and V. Apkarian, Chem. Phys. Lett. **218**, 504 (1994).
[10] R. Zadoyan, Z. Li, C. Martens, and V. Apkarian, J. Chem. Phys. **101**, 6648 (1994).
[11] U. Banin and S. Ruhman, J. Chem. Phys. **98**, 4391 (1993).
[12] U. Banin, R. Kosloff, and S. Ruhman, Chem. Phys. **183**, 289 (1994).
[13] T. Kühne and P. Vöhringer, J. Chem. Phys. **105**, 10788 (1996).
[14] I. Benjamin and R. M. Whitnell, Chem. Phys. Lett. **204**, 45 (1993).
[15] A. E. Johnson, D. E. Levinger, and P. F. Barbara, J. Phys. Chem. **96**, 7841 (1992).
[16] D. A. V. Kliner, J. C. Alfano, and P. F. Barbara, J. Chem. Phys. **98**, 5375 (1993).
[17] P. K. Walhout, J. C. Alfano, K. A. M. Thakur, and P. F. Barbara, J. Phys. Chem. **99**, 7568 (1995).
[18] I. Benjamin, P. Barbara, B. Gertner, and J. Hynes, J. Phys. Chem. **99**, 7557 (1995).
[19] H. Rosen, Y. R. Shen, and F. Stenman, Mol. Phys. **22**, 33 (1971).
[20] W. Kiefer and H. J. Bernstein, J. Raman Spectrosc. **1**, 417 (1973).
[21] J. Put, G. Maes, P. Huyskens, and Th. Zeegers-Huyskens, Spectrochim. Acta A **37**, 699 (1981).
[22] B. Cohen and S. Weiss, J. Chem. Phys. **72**, 6804 (1980); **74**, 3635 (1981).
[23] R. Sension and H. L. Strauss, J. Chem. Phys. **86**, 6665 (1987).
[24] M. Besnard, N. Del Campo, R. M. Cavagnat, and J. Lascombe, Chem. Phys. Lett. **162**, 132 (1989).
[25] C. A. Langhoff, K. Gnadig, and K. B. Eisenthal, Chem. Phys. **46**, 117 (1980).
[26] E. F. Hilinski and P. M. Rentzepis, J. Am. Chem. Soc. **107**, 5907 (1985).
[27] E. Lenderink, K. Dupen, and D. A. Wiersma, Chem. Phys. Lett. **211**, 503 (1993).
[28] L. A. Walker II, S. Pullen, B. Donovan, and R. J. Sension, Chem. Phys. Lett. **242**, 177 (1995).
[29] S. Pullen, L. A. Walker II, and R. J. Sension, J. Chem. Phys. **103**, 7877 (1995).
[30] E. Lenderink, K. Duppen, F. P. X. Everdij, J. Mavri, R. Torre, and D. A. Wiersma, J. Phys. Chem. **100**, 7822 (1996).
[31] S. J. Rand and R. L. Strong, J. Am. Chem. Soc. **82**, 5 (1960).
[32] R. L. Strong, S. J. Rand, and J. A. Britt, J. Am. Chem. Soc. **82**, 5053 (1960).
[33] R. L. Strong and J. Perano, J. Am. Chem. Soc. **83**, 2843 (1961).
[34] K. D. Raner, J. Lusztyk, and K. U. Ingold, J. Phys. Chem. **93**, 564 (1989).
[35] G. DeBoer, J. W. Burnett, and M. A. Young, Chem. Phys. Lett. **259**, 368 (1996).
[36] G. DeBoer, J. W. Burnett, A. Fujimoto, and M. A. Young, J. Phys. Chem. **100**, 14882 (1996).
[37] Y. Danten, B. Guillot, and Y. Guissani, J. Chem. Phys. **96**, 3782 (1992).
[38] R. J. Sension and H. L. Strauss, J. Chem. Phys. **85**, 3791 (1986).
[39] C. M. Chen and W. E. Wentworth, J. Phys. Chem. **89**, 4099 (1985).
[40] E. M. Voight, J. Phys. Chem. **72**, 3300 (1968).
[41] T. D. McLean, B. B. Ratcliff, J. Z. Pastalan, and K. K. Innes, J. Quant. Spectrosc. Radiat. Transf. **42**, 445 (1989).
[42] J. C. Schug and M. C. Dyson, J. Chem. Phys. **58**, 297 (1973).
[43] E. Kochanski and J. Prissette, Nouv. J. Chim. **4**, 509 (1980).
[44] I. Jano, Theor. Chim. Acta **66**, 341 (1985).
[45] R. M. Keefer and L. J. Andrews, J. Am. Chem. Soc. **77**, 2164 (1955).
[46] B. B. Bhowmik and S. P. Chattopadhyay, Spectrochim. Acta A **37**, 135 (1981).
[47] J. A. Joens, J. Org. Chem. **54**, 1126 (1989).
[48] V. P. Shedbalkar and S. N. Bhat,Bull. Chem. Soc. Jpn. **57**, 852 (1984).
[49] GAUSSIAN 94, Revision B. 3, M. J. Frisch *et al.*, Gaussian, Inc., Pittsburgh, Pennsylvania, 1995.
[50] H. McConnell, J. S. Ham, and J. R. Platt, J. Chem. Phys. **21**, 66 (1953); J. McHale, A. Banerjee, and J. Simons, *ibid.* **69**, 1406 (1978).
[51] P. Y. Cheng, D. Zhong, and A. H. Zewail, Chem. Phys. Lett. **242**, 369 (1995).
[52] P. Y. Cheng, D. Zhong, and A. H. Zewail, J. Chem. Phys. **103**, 5153 (1995).
[53] Note that there are several typographical errors in Ref. 38, Sec. IV A. Equation (4.9) should read $a_\nu=\{-x+s\ \ln x+(2\gamma-\nu)-(2\gamma-\nu-\frac{1}{2})\ln(2\gamma-\nu)\}$. Equation (4.10) should read $B^S_\nu=[\nu!]^{1/2}\ \exp(a_\nu/2)L^S_\nu(x)$ and Eq. (4.12) should read $|\nu\rangle=[\beta s/\sqrt{2\pi}]^{1/2}B^s_\nu(x)$.
[54] N. Pugliano, A. Z. Szarka, S. Gnanakaran, M. Triechel, and R. M. Hochstrasser, J. Chem. Phys. **103**, 6498 (1995).